# Carbonyl-based Redox-active Compounds as Organic Electrodes for Batteries: Escape from Middle-high Redox Potentials and Further Improvement?

*Fanny Lambert,[a,b] Yann Danten [c], Carlo Gatti, [d] Bryan Bocquet, [a] Alejandro A. Franco, [a,e,f] and Christine Frayret*[a,e]*

[a] Laboratoire de Réactivité et Chimie des Solides (LRCS), UMR CNRS 7314, Université de Picardie Jules Verne, Hub de l'Energie, 15 Rue Baudelocque, 80000 Amiens Cedex France. Réseau sur le Stockage Electrochimique de l'Energie (RS2E), FR CNRS 3459, France. *E-mail: christine.frayret@u-picardie.fr.

[b] The French Environment and Energy Management Agency (ADEME), 20 avenue du Grésillé- BP 90406, 49004 Angers Cedex 01 France.

[c] Institut des Sciences Moléculaires, UMR CNRS 5255, 351 Cours de la Libération, 33405 Talence, France.

[d] CNR SCITEC, CNR Istituto di Scienze e Tecnologie Chimiche "Giulio Natta", Sede Via C. Golgi, 19,20133 Milano, Italy.

[e] ALISTORE-European Research Institute, Hub de l'Energie, FR CNRS 3104, 15 rue Baudelocque, 80039 Amiens, France

[f] Institut Universitaire de France, 103 boulevard Saint Michel, Paris 75005, France

**Potential Energy Surfaces (PES) of A molecules interacting with Li**

The evolution as a function of the angle α (*i.e.* (C-C-Li)) of the calculated PES of A0 interacting with $Li^+$ is displayed in Fig. S1. It demonstrates the existence of at least three local energy minimum (planar) conformations (cf). The most stable complex forms a nearly bidentate interaction of $Li^+$ with both O-atoms of the A0 molecule whereas the two other ones can both be classified as monodentate structures involving only the interaction of $Li^+$ with the C=O group of A0.

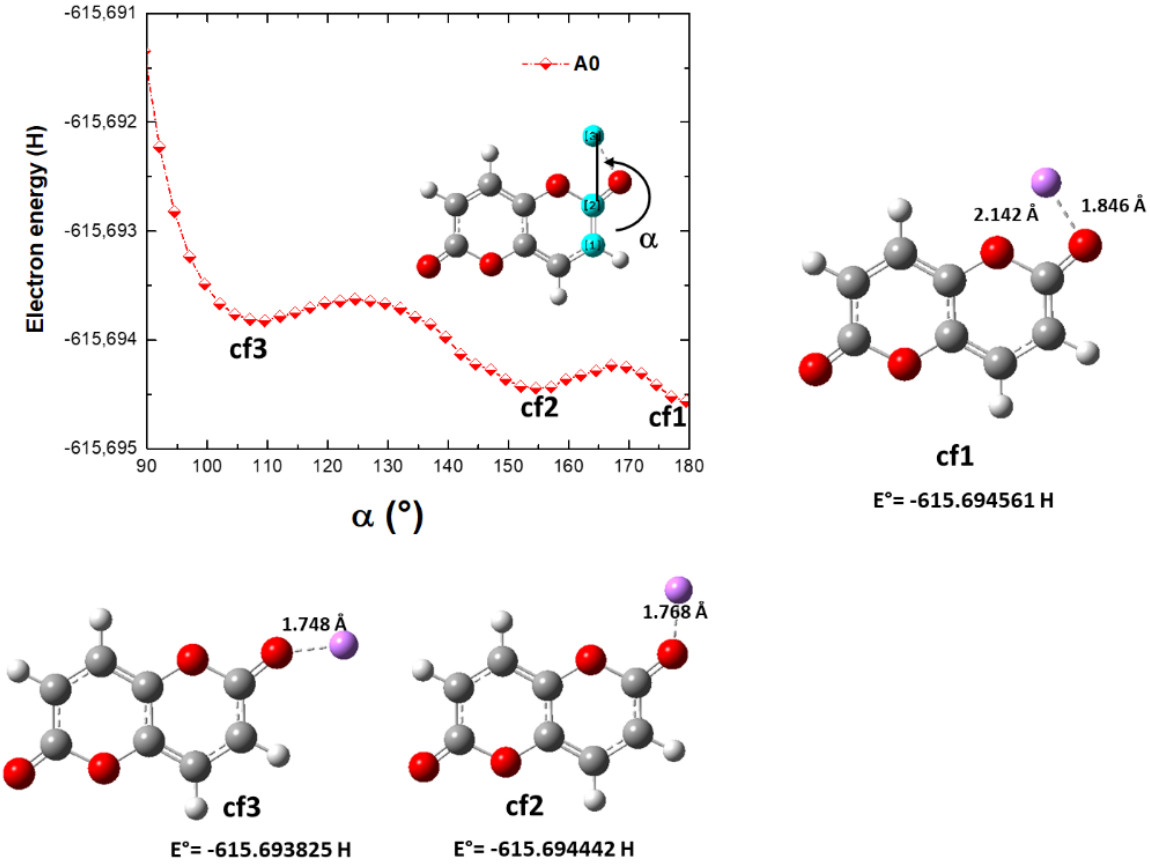


**Fig. S1: Evolution as a function of the angle α=(C-C-Li) of the PES of A0 interacting with $Li^+$ (intermediate form).**

A further examination of the PES of the complex between $Li^+$ and the A0 molecule, in particular with respect to the evolution with the angle (C,O,Li) formed between the C=O group of A0 with $Li^+$ (figure not shown), reveals the existence of another secondary structure (among possible other ones), which is significantly less stable. In this latter case, $Li^+$ is placed above the C-C bond of the PPD ring (Fig. S2).

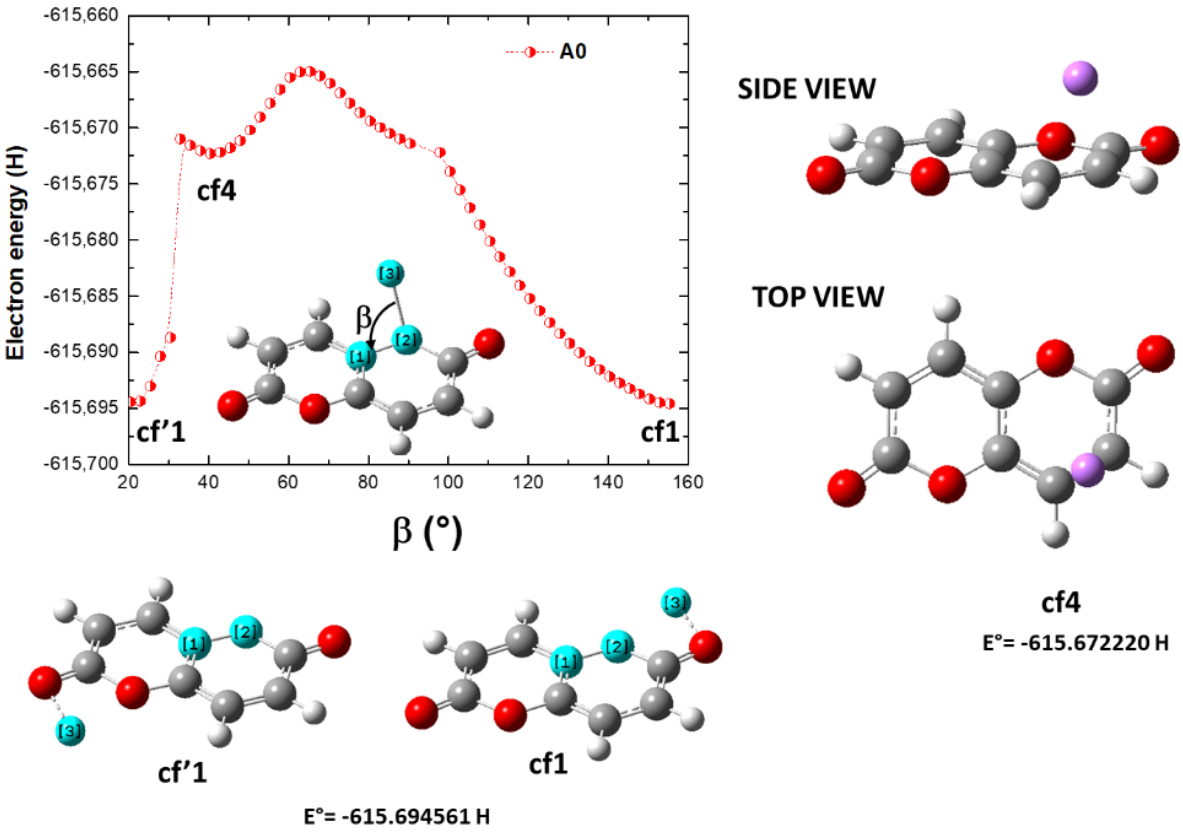


**Fig. S2: Presentation of the secondary local energy minimum structure (cf4) for the complex between $Li^+$ and A0, determined from the evolution of the PES as a function of the angle β=(C,C,Li).**

From exhaustive PES analyses carried out for the various Li-complexes formed with A1 and A3 molecules, it can be demonstrated that obtained results are similar. They confirm the existence of three local energy minimum (planar) structures in both cases (Fig. S3a and S3b).

a)

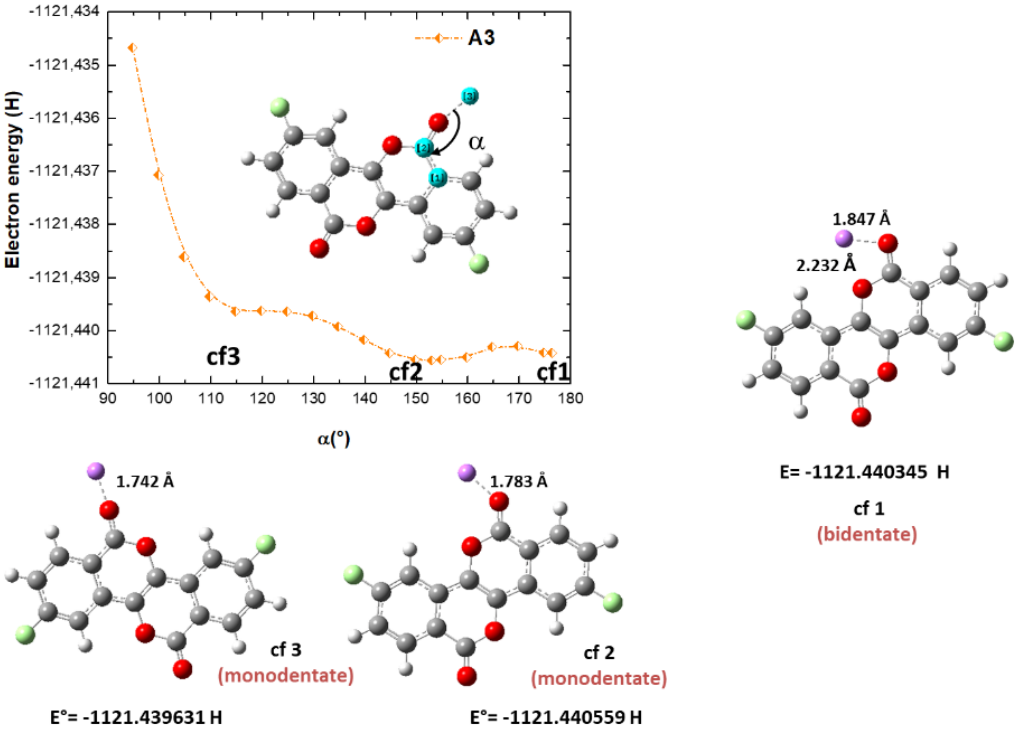


b)

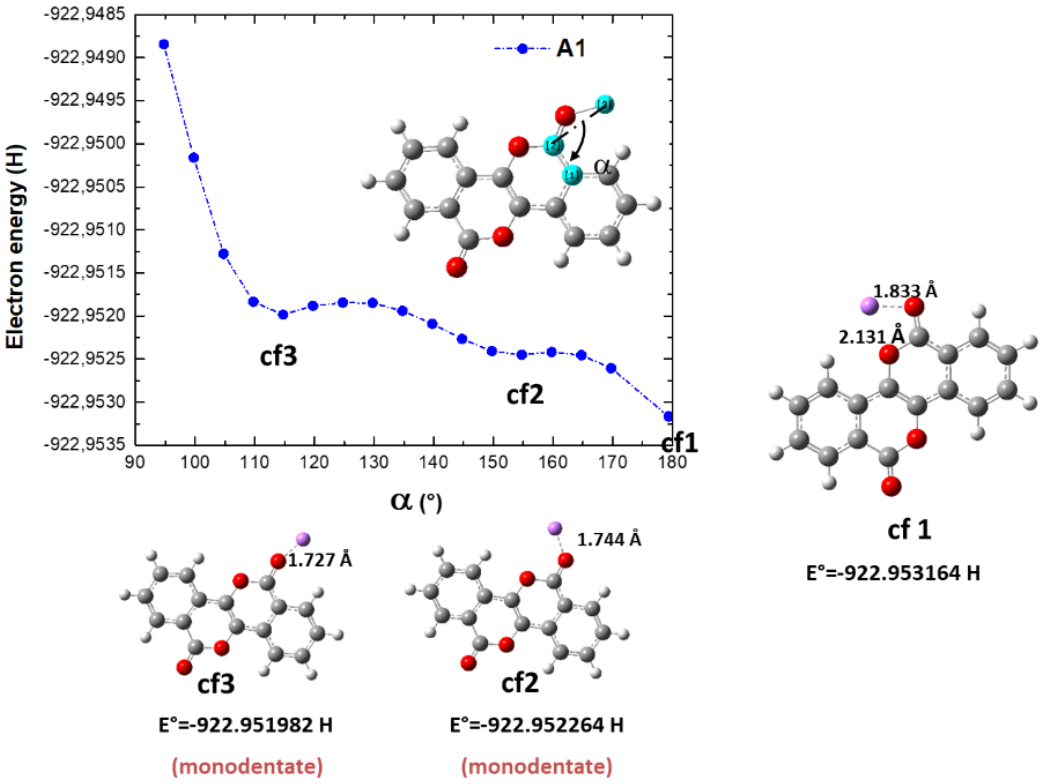


**Fig. S3: Evolution as a function of the angle α=(C-C-Li) of the PES of a) A1 and b) A3 molecules interacting with $Li^+$ cation (intermediate form).**

First, it can be inferred from the PES analysis of the complex between A1 and $Li^+$ that the benzene rings fused to the A0 central unit has no significant effect on the position of $Li^+$ with respect to the O-atoms of the A1 molecule. The Fluorine substitution of an H-atom on the benzene rings involved in the A3 molecule – thus inducing a withdrawing electronic effect of the halogen atom on both benzene rings – leads to the occurrence of a monodentate structure (cf2) for the complex between A3 and $Li^+$, which is now the most stable one. We can notice that the energy differentiation comparatively to the two other conformations (and more specifically with respect to the bidentate structure cf1) is rather weak.

The study of the interaction between $Li^+$ and the A5/A5_ext molecules enables the evaluation of the influence of fused thiophene rings/fused benzene and thiophene rings. Fig. S4 displays the evolution as a function of the angle α =(C-O-Li) of the calculated PES for the A5 molecule interacting with $Li^+$. It demonstrates that it exists now only two distinct local energy minimum (planar) structures characterizing the interaction between A5 and $Li^+$ (Branch 1). Another structure (although less stable) has also been identified, in which $Li^+$ interacts with the sulphur atom of the thiophene ring of the A5 molecule (Branch 2).

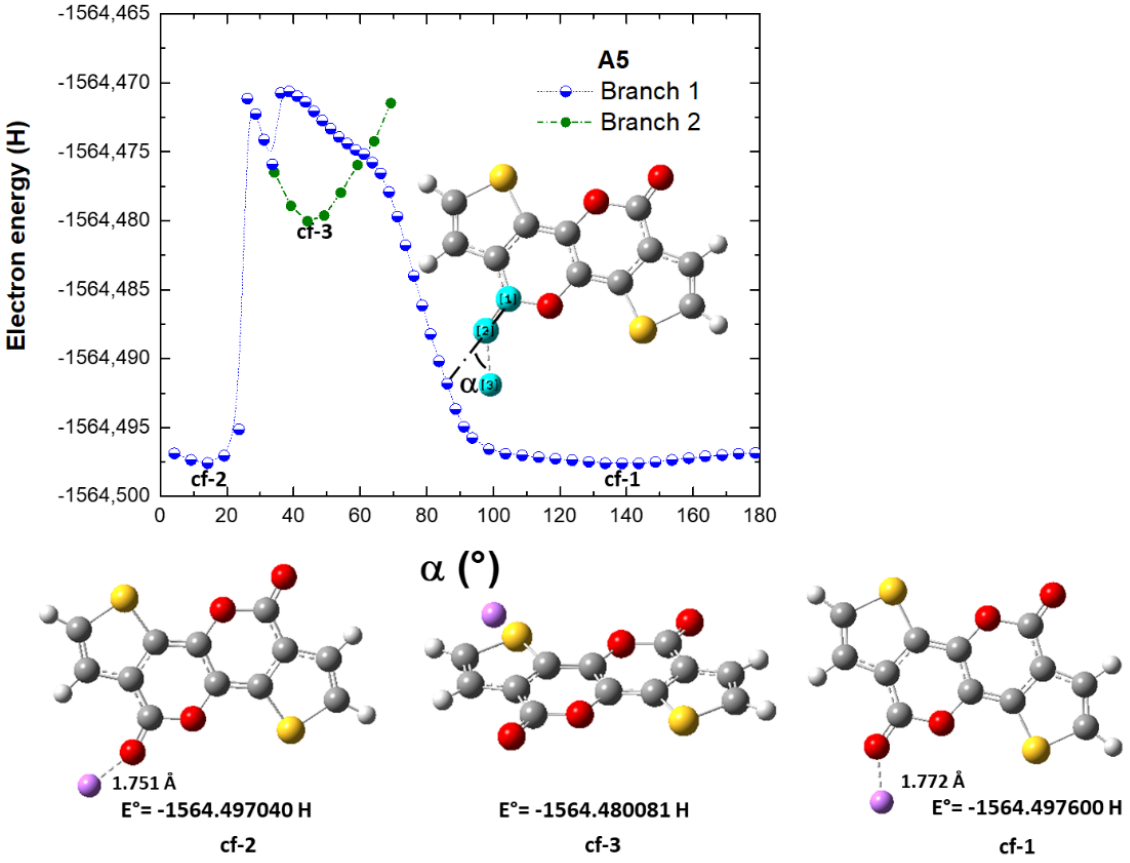


**Fig. S4: Evolution as a function of the angle α=(C-O-Li) of the PES for the complex between $Li^+$ and A5 (intermediate form).**

In the same way, Fig. S5 displays the evolution as a function of the angle α=(C-O-Li) of the calculated PES for the A5_ext molecule interacting with $Li^+$. It exists only two distinct local energy minimum (planar) structures (cf1 and cf2) involving monodentate interaction with $Li^+$. A further PES analysis of the non-planar conformation of A5_ext interacting with $Li^+$ allows the determination of a third structure (cf3), which is less stable. In this latter, $Li^+$ interacts with the sulphur atom of the thiophene ring. From the location of the Transition State (TS) structure (local stationary point of the first order type) associated with the conformational transition between both structures (cf1 and cf3) – in which $Li^+$ is situated above the benzenic ring of the A5_ext molecule – Integrated Reaction Coordinate (IRC) Path were then evaluated. The Gibbs energy barrier to cross in order to go from structure cf1 to structure cf3 is estimated at about 13.3 kcal/mol (Fig. S6). In contrast, the reverse transformation from the structure cf3 to structure cf1 exhibits a height of barrier significantly lower than the former one, evaluated at 1.3 kcal/mol. This result suggests that the interactions of $Li^+$ above the sulphur atom from thiophene ring is poorly favoured compared to the planar structures.

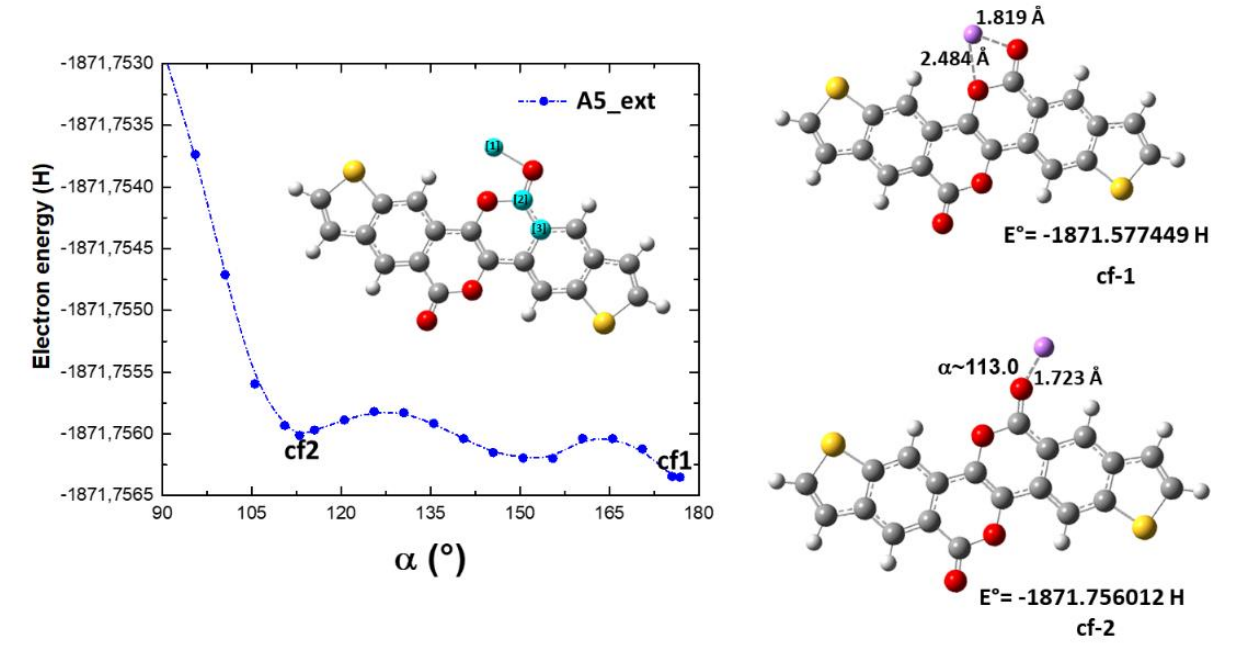


**Fig. S5: Evolution as a function of the angle α=(C-O-Li) for the PES the complex between $Li^+$ cation and A5_ext (intermediate form).**

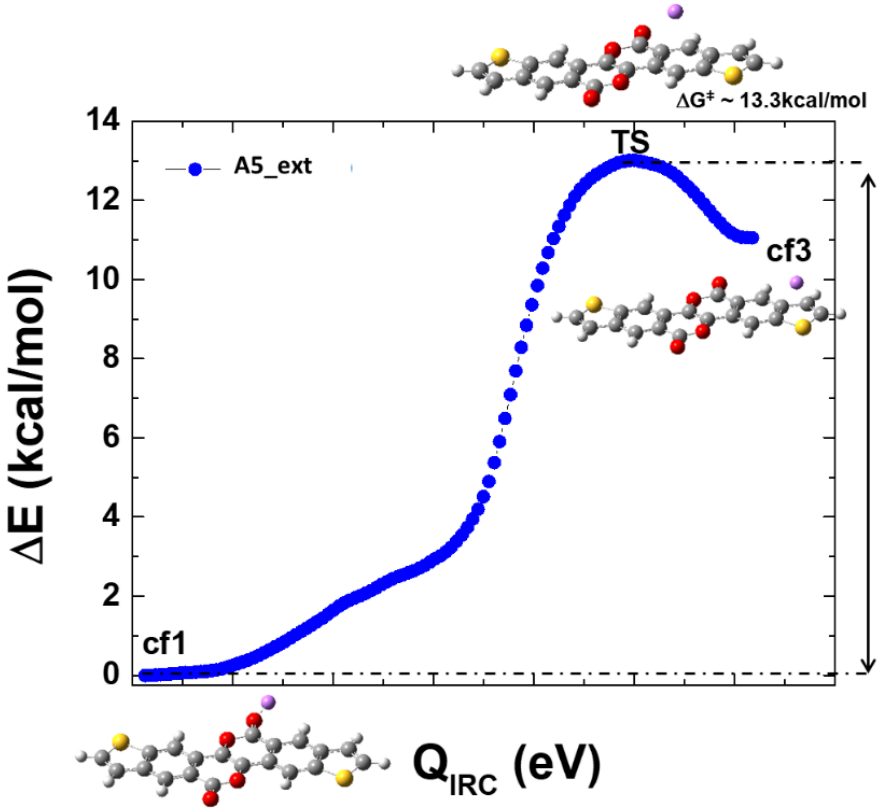


**Fig. S6: Calculated Integrated Reaction Path between cf1 and cf3 conformations of the A5_ext compound interacting with $Li^+$ cation (intermediate form). The Transition State structure allows the estimation of the barrier height for this conformational transition (~13.3 kcal/mol).**

In the case of Na-electrochemistry, the most stable structures of both singly and doubly reduced A-systems correspond preferentially to bidentate cases involving interactions between $Li^+$ and oxygen atoms belonging to the carbonyl group and to the nearby ring of the molecule.

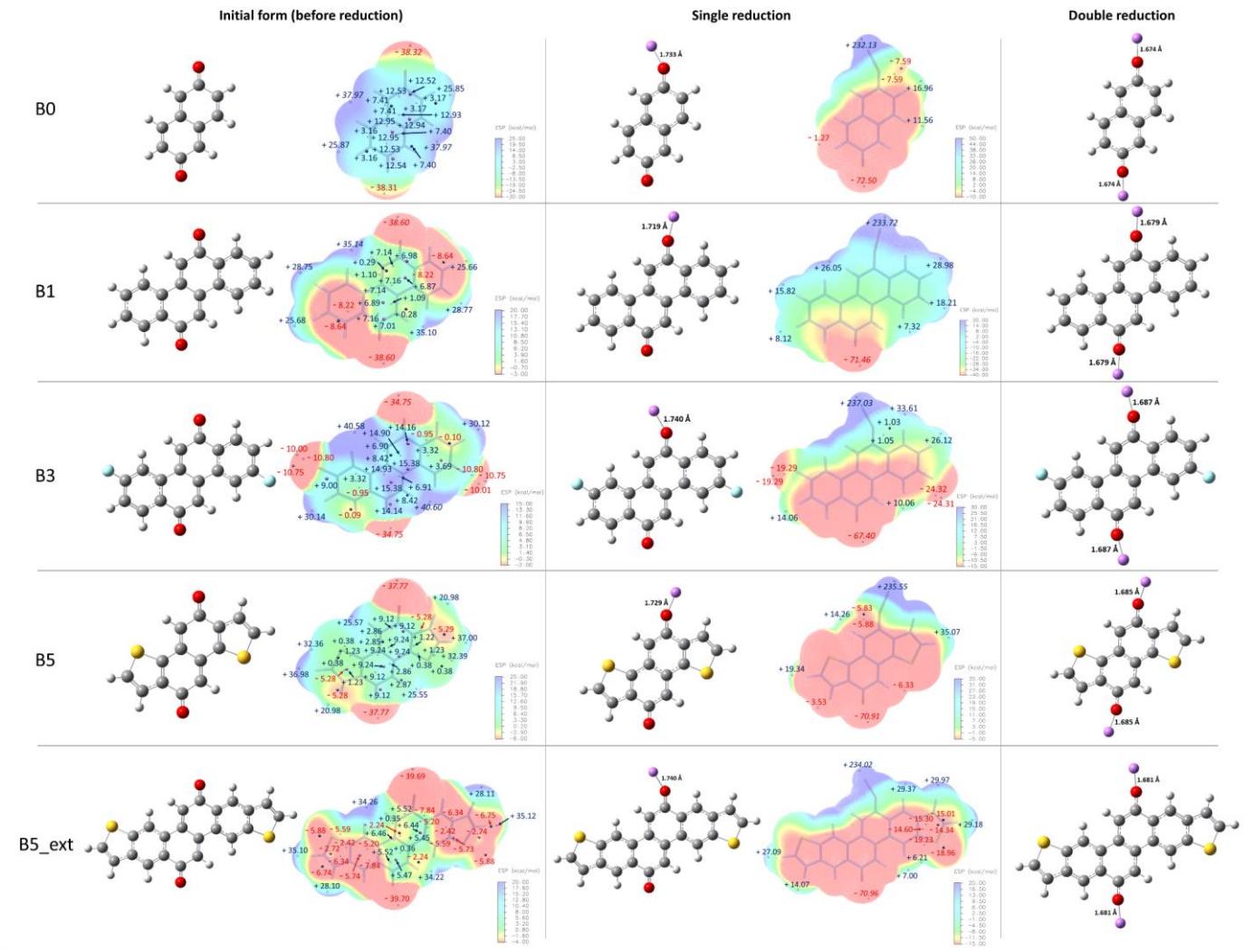


**Fig. S7: ESP maps and structures for the initial, intermediate and final forms of the most stable Li-based B PPD-derivatives (scales in kcal/mol). Left: monomer (initial state); Middle: complex involving one $Li^+$ cation (single reduction); Right: complex involving two $Li^+$ cations (double reduction).**

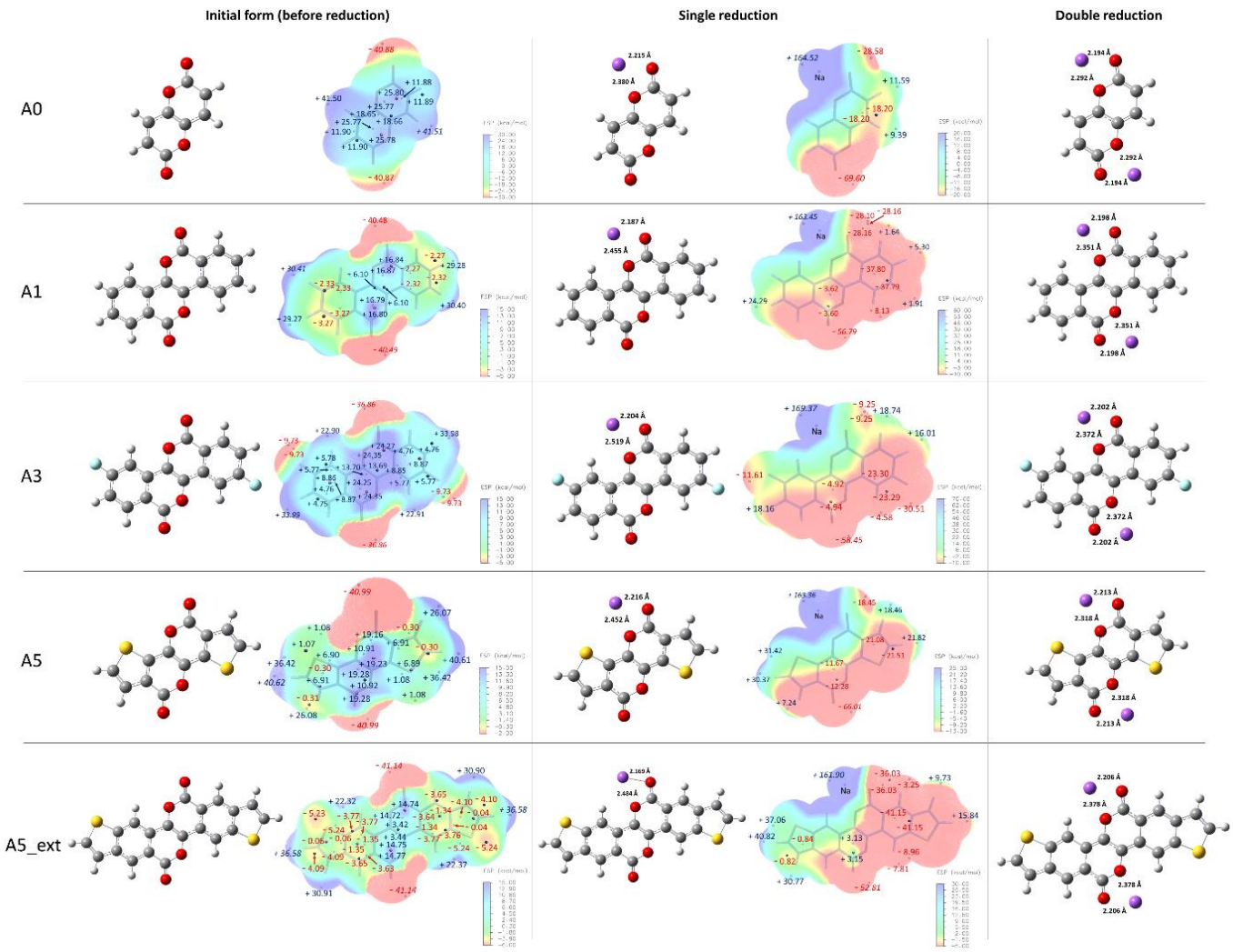


**Fig. S8: ESP maps and structures for the initial, intermediate and final forms of the most stable Na-based A PPD-derivatives (scales in kcal/mol). Left: monomer (initial state); Middle: complex involving one $Na^+$ cation (single reduction); Right: complex involving two $Na^+$ cations (double reduction).**

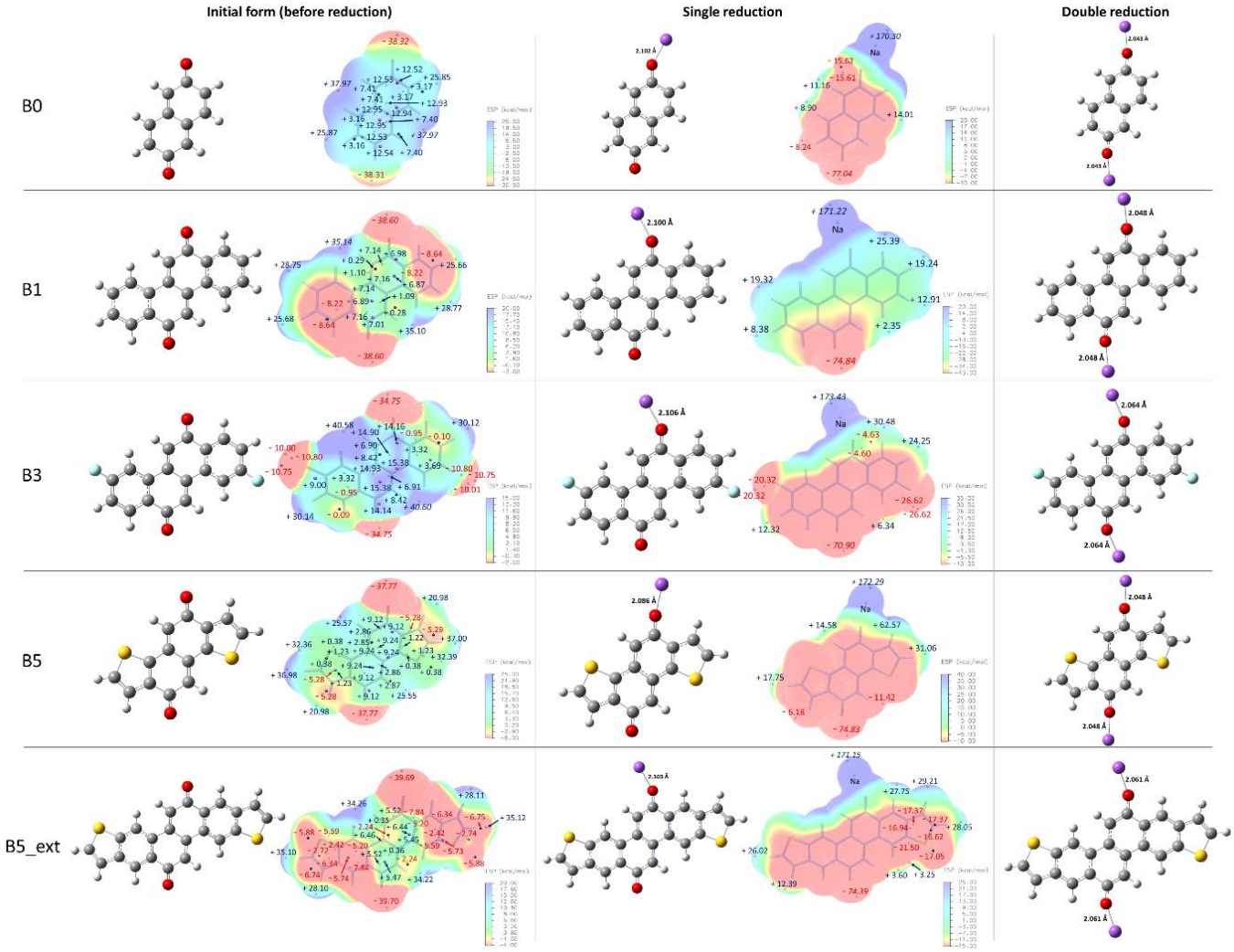


**Fig. S9: ESP maps and structures for the initial, intermediate and final forms of the most stable Na-based B PPD-derivatives (scales in kcal/mol). Left: monomer (initial state); Middle: complex involving one $Na^+$ cation (single reduction); Right: complex involving two $Na^+$ cations (double reduction).**

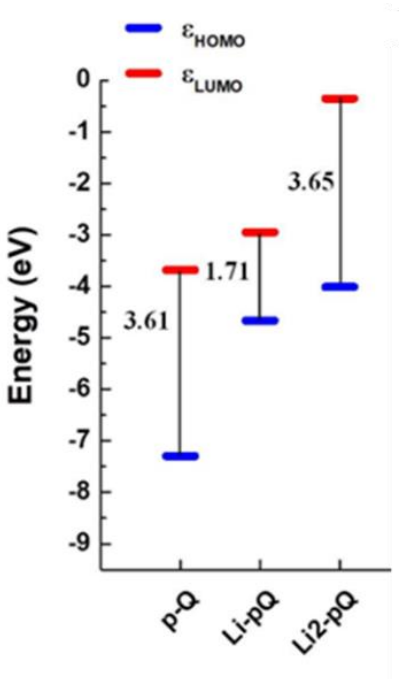


**Fig. S10: Calculated HOMO/SOMO and LUMO energy levels and corresponding gaps (in eV) of *para*-benzoquinone (*p*-BQ) for the molecular state, Li-single reduction and Li-double reduction.**

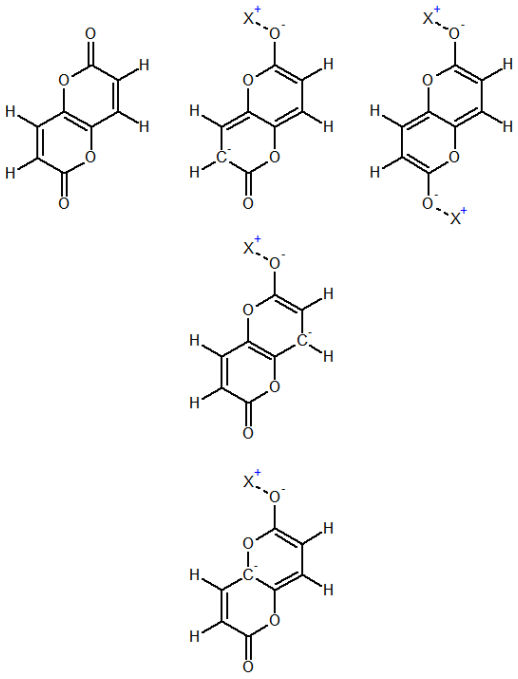

**Fig. S11: Resonance structures of A0 in initial (left), intermediate (middle) and final (right) states.**

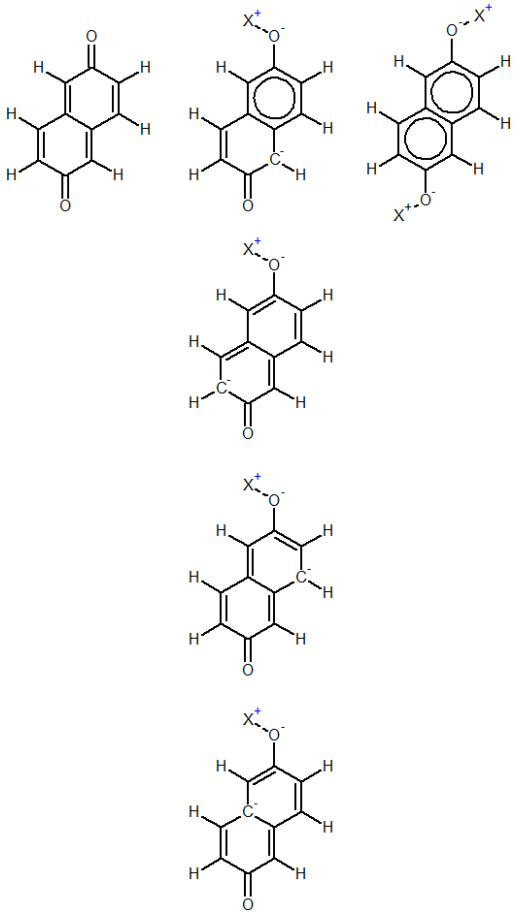

**Fig. S12: Resonance structures of B0 in initial (left), intermediate (middle) and final (right) states.**

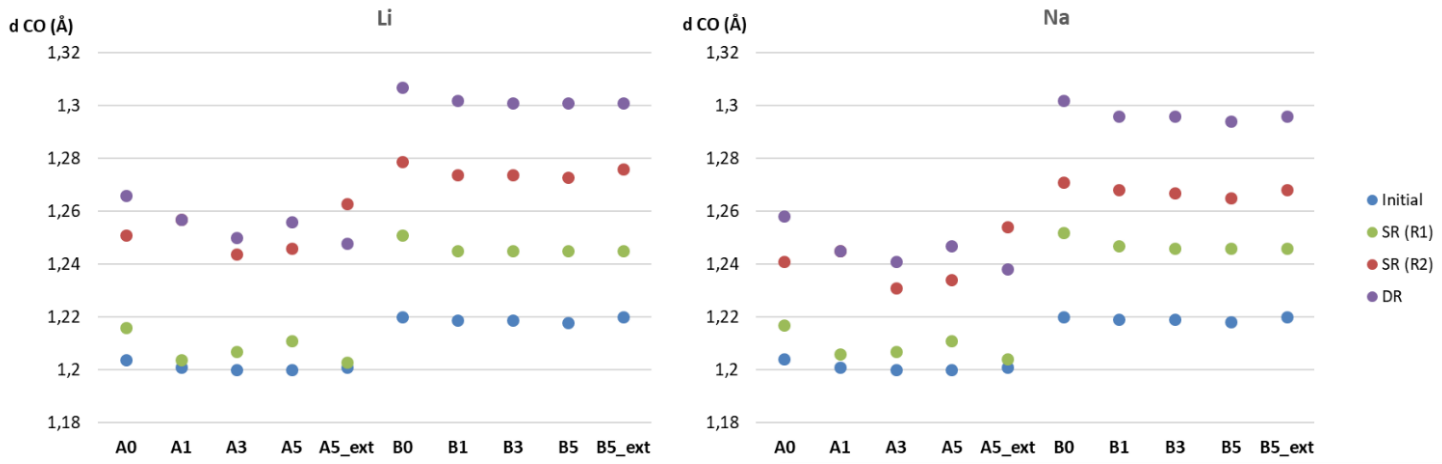


**Fig. S13: Interatomic distances, d (in Å), between the oxygen atom and the carbon atom, both belonging to the carbonyl group.**

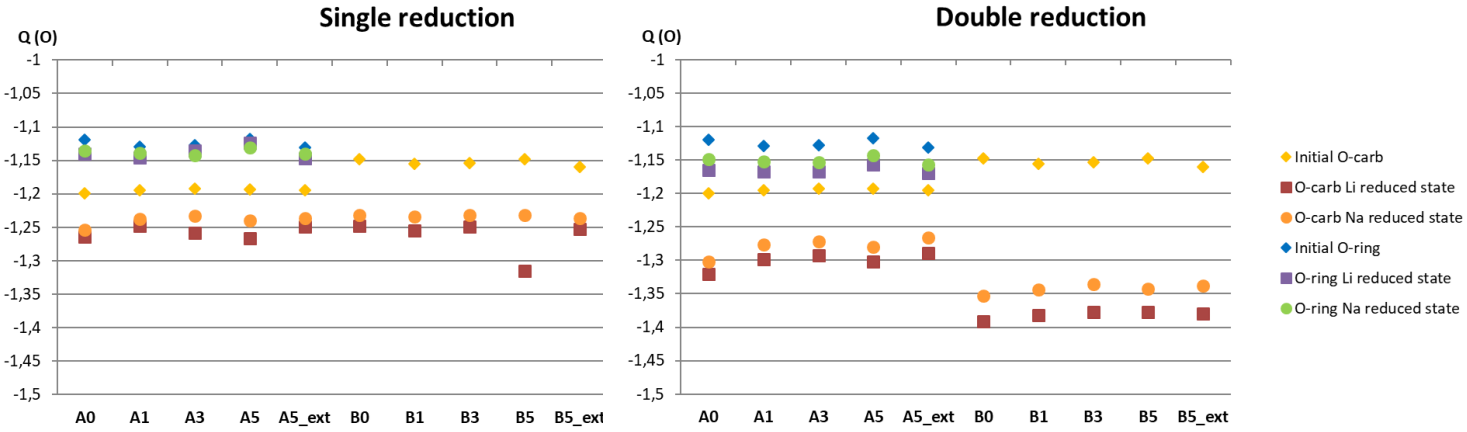


**Fig. S14: Bader's net atomic charge (NAC) average (Q) values for either the two Oxygen atomic species belonging either to the carbonyl groups or to the two ones belonging to the rings. Values provided in the initial, intermediate and final states, for both Li- and Na-insertion.**

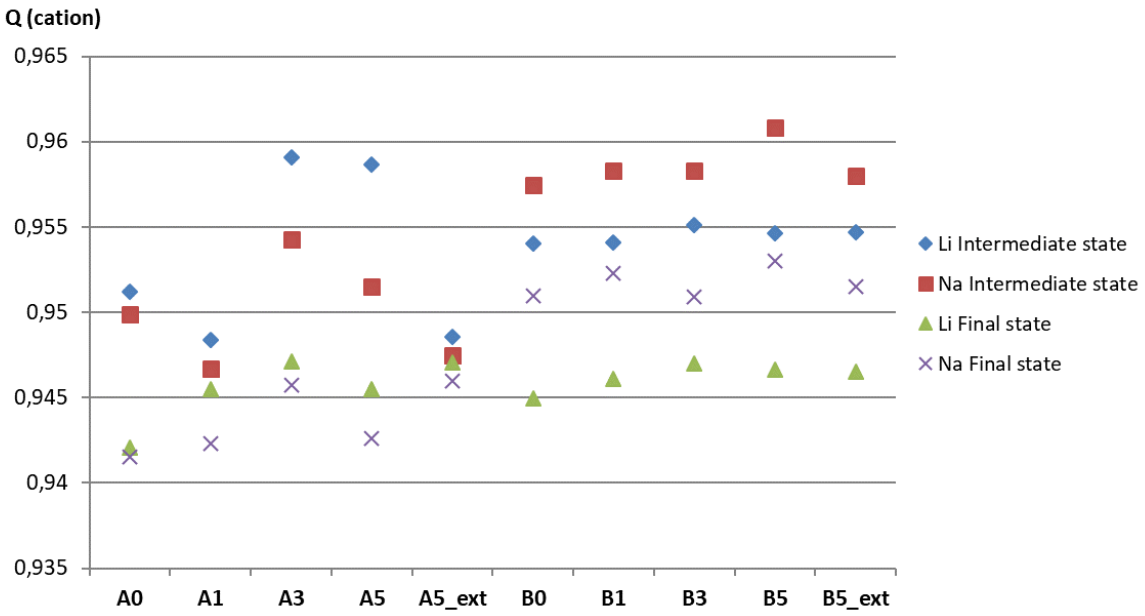


**Fig. S15: Bader's net atomic charge (NAC) average values (Q) for the inserted $Li^+$ and $Na^+$ cations in the intermediate and final states.**

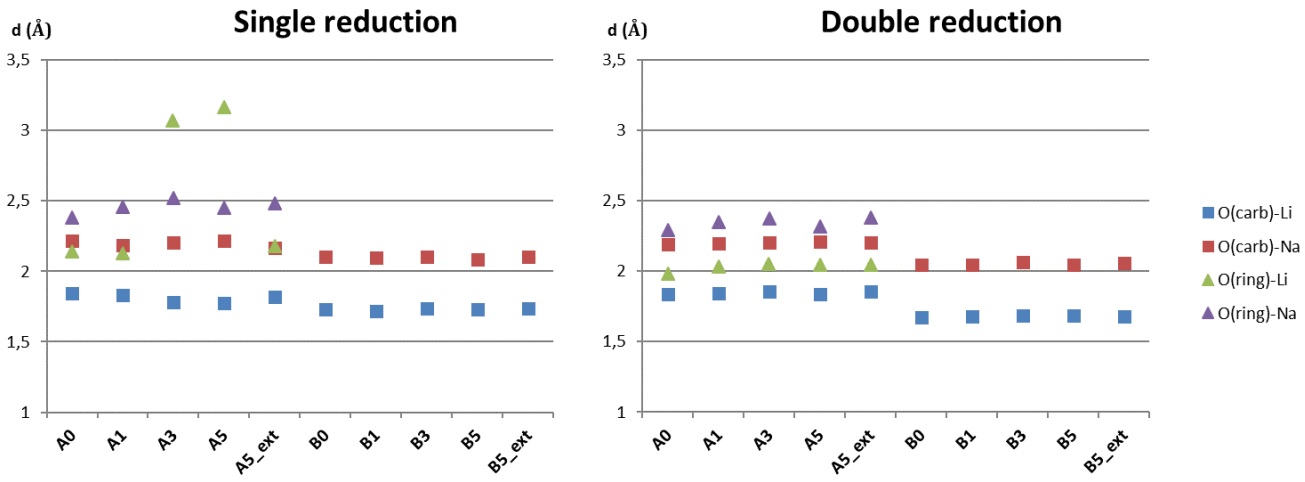


**Fig. S16: Interatomic distances, d (in Å), between the oxygen atoms (either belonging to the carbonyl group or to the rings) and the alkali metal cation, for one-electron (left) and two-electron (right) process.**